3
Experimental Details

There are various synthesis techniques, which can be used for fabricating spectrally selective structures, as reviewed in chapter 2. This chapter will discuss in detail about the experimental techniques used for the synthesis of spectrally selective coatings, used in this thesis work. Section 3.1 includes the electrochemical deposition and DC/RF magnetron sputtering processes. These spectrally selective absorber coatings are further characterized to understand the structure and microstructure, constituent elements, thickness of coatings, optical properties such as absorptance and emittance, mechanical and corrosion properties. Further, thermal stabilities of these structures have also been investigated using thermal gravimetric analysis and cyclic heating. The details of characterization techniques, used for this work, are described in section 3.2.

3.1 SAMPLE PREPARATION TECHNIQUES

3.1.1 Electrochemical Deposition

The electrochemical deposition, also known as electrodeposition, is one of the metal and alloys thin film deposition techniques. In this technique, ions from electrolytic (aqueous, organic and fused- salt) solutions are reduced and transferred in the presence of an electric field to form a film on the desired substrate. The electrodeposition cell consists of an anode, cathode, and electrolyte. Furthermore, anodes are divided into two categories: one is sacrificial and another is a permanent anode. The sacrificial anodes are to be deposited and the permanent anode is employed to complete the electrical circuit and does not participate in the electrochemical process. An electrolyte is the ionic conductor, which allows ions to transport from one electrode to another instead of free electrons to complete the internal electrical circuit. After applying bias/electrical potential, the cations and anions in the electrolyte will move towards the cathode and anode. Moreover, ions conduct through the electrolyte to draw the electrical current in the internal circuit, which is complemented by an equivalent electronic current in the external circuit. The metallic cations are attracted towards the cathode through the electrolyte, where excess electrons on the cathode (workpiece) neutralize the cations into metallic ones. These reduced cations form a metallic film on the surface of this negatively charged workpiece (i.e. cathode) [Paunovic and Schlesinger, 2006; Lou and Huang, 2006]. The electrochemical setup is illustrated schematically in Figure 3.1 (a). The system is kept on a hot plate to achieve the desired temperature during electrodeposition process and connected with DC power supply to provide the desired voltage/current for potentiostatic/galvanostatic electrodeposition process. The actual experimental setup is shown in Figure 3.1(b), which is used to deposit spectrally selective absorber films on different substrates such as stainless steel, copper, and aluminum etc. in the present work.

Redox (reduction/oxidation) reactions are electron transfer reactions in the electrolysis process. The electrode, gaining electrons, oxidizes another electrode, which is losing electrons in the process. Cations are reduced at cathode accepting electrons, which flow towards the anode (Equations (3.1) & (3.2)).

$$M^{n+} + ne^- \rightarrow M \quad (3.1)$$

$$M \rightarrow M^{n+} + ne^- \quad (3.2)$$

The electrodeposition of metal oxides is mainly performed in alkaline aqueous solutions containing metal complexes under oxidizing and reducing conditions. In each case, the metal ions dissociate from metal complexes and precipitate on the electrode as oxide and process can be explained in two steps. The first step is the metal dissolution, which is an electrochemical process (3.2). The second step is the chemical process between metal and hydroxide ions on the surface of the substrate.

$$M^{n+} + OH^{n-} \rightarrow M(OH)_n \quad (3.3)$$

The electrodeposited oxides may consist of complex compositions such as metal alloys, metal oxide, and metal hydroxides. Further, controlled heat treatment can be used to convert such composites into the desired composition for probable applications.

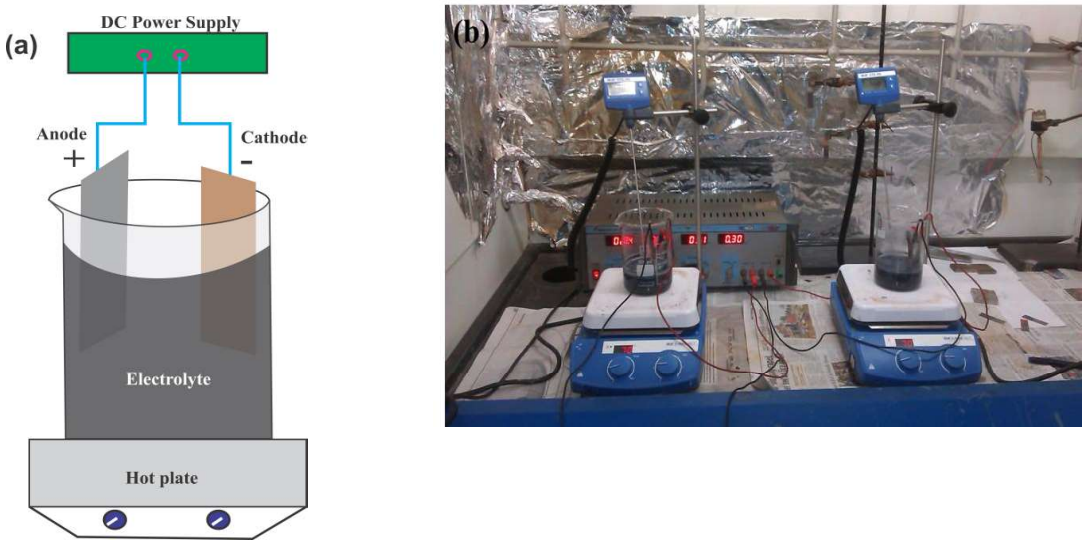

Figure 3.1 : (a) Schematic diagram of experimental setup for electrodeposition. **(b)** Electrochemical deposition experimental setup in our lab used to deposit spectrally selective absorber films.

3.1.2 RF/DC Sputtering Technique

Sputtering is a physical deposition process, where materials (neutral atoms or molecules) are etched from a solid surface, known as the target (due to the transfer of momentum between an energetic gas particle (ions), and the target surface). Grove was the first one, who observed the sputtering process in a dc gas discharge tube in 1852, and now this process is frequently used to deposit the desired thin film structures.

The important parameter for sputtering process is the yield (ratio of number of ejected atoms to number of bombarding ions) of the sputtered materials. This is the function of chemical binding of the target material and collision energy impact. There are two types of sputtering sources, one is glow discharge source and another is an ion beam source. The following section discusses glow discharge sputtering, and RF/DC magnetron sputtering

processes. Different types of sputtering systems are developed for thin film depositions. Among them, the first one is the dc diode sputtering system and others are the advancement of this dc diode sputtering system [McClanahan and Laegreid, 1991].

3.1.2.1 DC Diode and Triode Sputtering

DC diode sputtering has a vacuum chamber with two electrodes, appropriate pumping, and the gas flow arrangement, as illustrated in Figure 3.2(a). The target material is fixed at the cathode, to be sputtered, and held at a negative potential. Substrates are placed on the anode. Positively charged Ar^+ ions are bombarded on the target, and ejected neutral target atoms/molecules are deposited onto the substrate [Shah, 1995]. An optimum gas density is required to maintain the glow discharge. In low gas density, electrons are impacted on the anode without ionizing any argon atom; however, at higher gas density electrons do not have sufficient energy to ionization argon atom. The secondary electrons, which are produced by the accelerated ions, play a major role to ionize atoms in the discharge. The main disadvantages of DC diode sputtering are low deposition rates, high gas densities, high discharge voltages, lack of versatility, and suitable for conducting targets only [Rossnagel, 1991]. A heated filament is used to inject electrons directly into the plasma to further enhance the ionization of plasma, as shown in Figure 3.2 (b), which enhances the electron density and thus, providing higher deposition rates. This is called the triode sputtering, because of additional electron source filament arrangement. The major problems with triode sputtering are (i) its' scaling up and (ii) gas species interaction with the filament, which may create impurities during deposition.

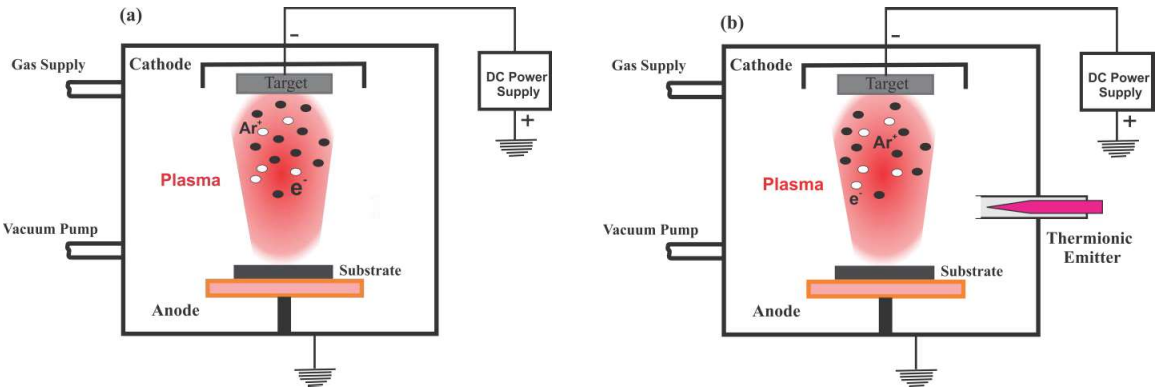

Figure 3.2 : Schematic of **(a)** DC diode sputtering system and **(b)** DC triode sputtering system. (Source: Waite *et al.*, 2010)

3.1.2.2 Radio Frequency (RF) Sputtering

RF sputtering is employed to produce insulating thin films and coatings such as dielectric oxide films [Davidse and Maisel, 1966; Davidse, 1967a, 1967b]. The mail limitations of a RF sputtering system are the high cost power supply and the complicated matching network, which is utilized to lower the reflected power during the sputtering process. A 13.56 MHz radio frequency power supply is used with impedance matching network and blocking capacitor, as illustrated in Figure 3.3. Electrons are oscillating between two electrodes with the frequency of applied power [Rossnagel, 1991]. A net negative DC bias is applied to attract the ions for sputtering and the resulting deposition of target materials on a desired substrate [Est and Westwood, 1998]. In RF sputtering, the capacitive coupled plasma is formed near the target, which makes no difference in the target surface whether the target is electrically conductive or insulating. However, RF sputtering rate of insulating materials is relatively poor due to the lower sputter yield of insulators. The power is divided between the two electrodes in RF

sputtering process and the RF sputtering power at the cathode is half of the power delivered in DC sputtering. This low effective power at the cathode is the main reason for low deposition rates in RF sputtering processes as compared to that in an equivalent DC process. The major problem with DC diode, triode, and RF sputtering systems is the nonuniform plasma densities, causing nonuniform current density and film thickness during the deposition process.

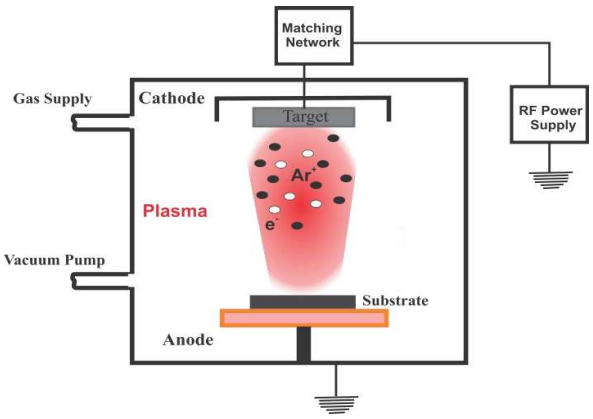

Figure 3.3 : Schematic diagram of an RF sputtering system, with respective legends. (Source: Waite *et al.*, 2010)

3.1.2.3 Magnetron Sputtering

In conventional sputtering, target is fixed with cathode plate and bombarded with energetic ions, produced in the available plasma. The target materials are etched out during bombardment process and settle down in the form of a film on the substrate. The secondary electrons, which are generated by the target at the time of bombardment, also play a crucial role in sustaining plasma during synthesis. However, conventional sputtering procedure has constraints like low deposition rate, low ionization capacity, and more substrate heating impacts. These constraints can be minimized by using the magnetron sputtering system in place of conventional DC and RF sputtering systems [Kelly and Arnell, 2000]. The confinement of electrons near the surface target can be increased with the help of magnetic field so that the plasma density increases in magnetron sputtering. The first demonstration of a magnetron sputtering was done by Penning in 1935. Further, Clark had developed a sputtering source, known as sputtering gun, in 1968, and J.S. Chapin designed a planar magnetron in 1974 and patented the same [Waite *et al.*, 2010].

(a) Planar Magnetrons

The arrangement of planar magnetron sputtering system is identical to that of DC and RF sputtering system. However, it has fixed magnetic arrangement at the back of the cathode to confine the electrons near and above the targets (Fig. 3.4 (a)) [Waits, 1978]. The orientation of magnetic field is radial and overhead the cathode. Hence, the **E** X **B** drift forms a circular path along the target. This localized nonuniformity creates a circular region on the target surface, which is known as the racetrack, resulted in poor utilization of target (20% to 45%). In the 1980s, Wright and Beardow, designed the rotatable cylindrical magnetron to solve the problem of low target utilization. Cylindrical magnetrons have been extensively employed in the coating of complex shaped substrates [Siegfried *et al.*, 1996]. Figure 3.4 (b) illustrate the cylindrical magnetrons, where the cathode is along the axis and anode a concentric tube. The inverted arrangement of the same is known as hollow magnetron.

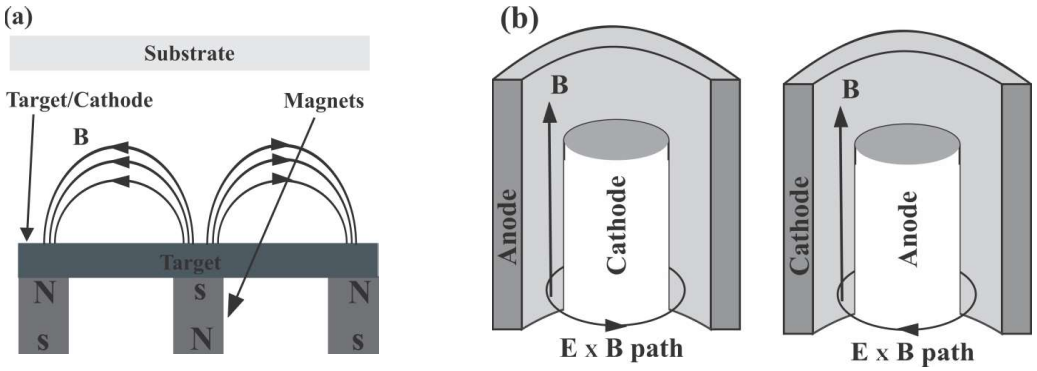

Figure 3.4 : Schematic diagram of **(a)** Planar Magnetron sputtering system and **(b)** Cylindrical Magnetron sputtering system. (Source: Waite *et al.*, 2010)

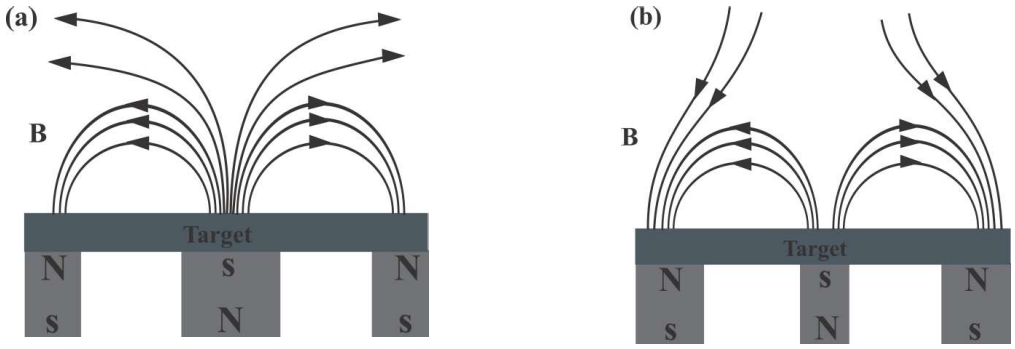

Figure 3.5 : Schematic diagram of **(a)** unbalanced Magnetron sputtering system type I and **(b)** type II. (Source: Waite *et al.*, 2010)

(b) Unbalanced Magnetrons

Keeping in mind the above said problems in planar/conventional magnetron sputtering, Window and Savvides developed a new design, known as an unbalanced magnetron in which different strength magnets are used. Employing the unbalanced magnetron sputtering system, could increase the ion bombardment on the target and thus growing films become denser and preferentially oriented [Pradhan and Shah, 2002]. There are two types of the unbalanced magnetron, Type I has a strong central magnet and Type II has strong outer magnets, as explained in Fig. 3.5 [Window and Savvides, 1986]. One of the major disadvantages of the unbalanced magnetron is that the plasma is not uniform, and thus may lead to the non-stoichiometry and non-uniform deposition in the final structures.

(c) Reactive Sputtering

The reactive sputtering process has been extensively investigated since 1980, due to the possibility of easily synthesis process for compound films, such as nitrides, oxides, carbides or their combinations, using conventional metal targets [Musil *et al.*, 2005]. Reactive sputtering of the metallic target with DC power supply is less expensive than RF power supply because of matching network and low yield with RF sputtering process. In reactive sputtering, gasses are in molecular state. Normally, reactive gasses have low atomic masses and do not contribute effectively in sputtering of the target atoms. That's why argon is used as sputtering gas in conjunction with a small fraction of reactive gas during the deposition process. The problems with reactive sputtering are the creation of a compound layer on the target itself and afterward target surface charging, which finally reduces the sputtering yield. The sputter rate decreases due to the conversion of target surfaces into respective insulating compounds, which is also

known as poisoning of the target surface. The detailed specification of a combined DC/RF sputtering system, which is used for the present work, described below.

The combined DC/RF sputtering system has a box type stainless steel vacuum chamber (process chamber), with 550 mm (width) x 450 mm (height) x 550 mm (length) dimensions. The inner view of this vacuum chamber (process chamber) is shown in Figure 3.6. A thin stainless steel sheet is used inside the chamber to prevent the deposition on the chamber walls. It has four water cooled 4" diameter magnetron sources, with an optimized inclination to include the 6" deposition region, as shown in Figure 3.6. (Arrows are marked for easy identification). Electro-pneumatically operated source shutter has been used with each magnetron source to open or close the required sputtering source during the sputtering process. The substrate holder is made of non-magnetic stainless steel material, integrated with a rotational mechanism. A substrate heater is placed below the substrate holder, which can be used to heat the substrates up to 800°C, using a digital PID controller in conjunction with a K-type thermocouple to measure the temperature.

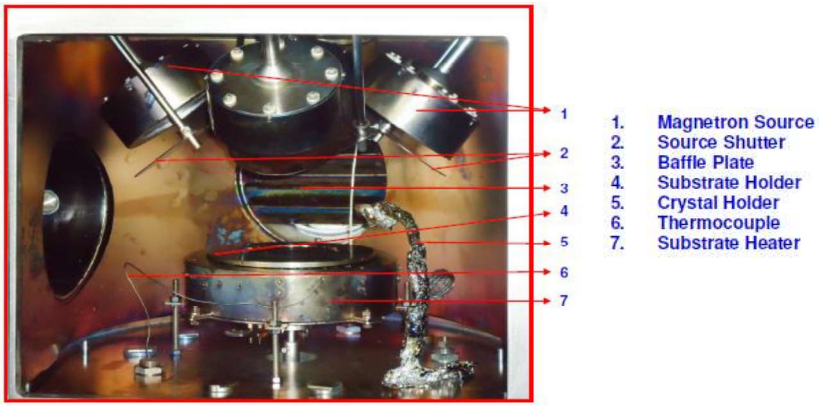

Figure 3.6: An inside view of the vacuum chamber (process chamber) of combined RF/DC magnetron sputtering system in our lab used to deposit spectrally selective absorber films.

A 400 (W) x 400 (D) x 450 (H) mm^3 box type 304 SS load lock chamber is integrated with the main deposition chamber. The inside view of load lock chamber is shown in Figure 3.7. A magnetic transfer mechanism with sample loading unit is used for transferring the substrate manually between the load lock and the process chamber. Linear positioning is controlled by sliding an external sleeve, which is magnetically coupled with transporters and sample holder inside the system.

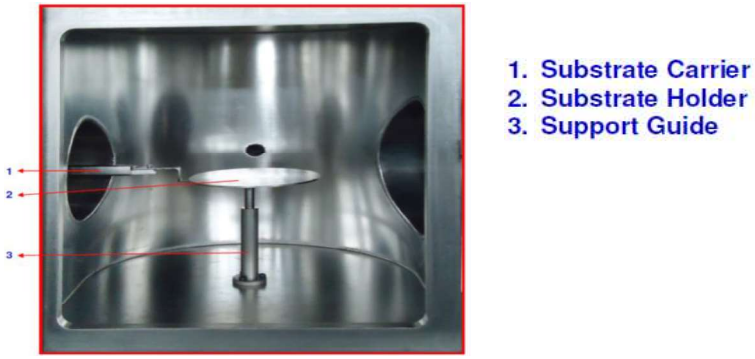

Figure 3.7: An inside view of load lock chamber of combined RF/DC magnetron sputtering system.

Two RF power supplies (at 13.56 MHz frequency and 600 watts maximum), make M/S. SEREN, USA, are installed with the sputtering system. This has an auto matching network, to feed RF power at resonance condition to the magnetron source during the thin film deposition process. In addition, two 2 kW DC power supplies are integrated with the system and can be used for DC sputter deposition. A 300 W, 13.56 MHz RF power supply, M/S, SEREN, the USA make, is available with the system for substrate biasing and pre-cleaning. This combined RF/DC sputtering system is configured with a direct drive rotary pump (model FD-60) having 1000 lit/min free air displacement capacity. Pump is fitted with an anti-suck back device to protect the system from back streaming of rotary pump oil during power failures. Leybold turbo molecular pump with model: TURBOVAC 1100C is configured with the system in line with a rotary pump. Figure 3.8 shows the front view of Hind High Vacuum (HHV) make RF/DC magnetron sputtering system.

Figure 3.8 : Front view of the combined RF/DC magnetron sputtering system.

3.2 HEAT TREATMENT

Heat treatment is a process, used in baking materials, at the desired heating rate and for a period of time. This can be used to change the properties of the materials as well. The objective of the heat treatment is to achieve the desired physical, chemical and mechanical properties etc. [Rajan *et al.*, 1992]. Thermal analysis related equipment, used to understand the thermal degradation of spectrally selective coatings in air and vacuum, is described later in characterization techniques section.

In this work, heat treatment processes have been explored to understand the materials response against the thermal treatment under both air and vacuum/inert conditions. For air treatment, a tabular furnace (Nabertherm GmbH), shown in Figure 3.9, has been used for annealing specially in air, wherever required for thermal treatment of spectrally selective coatings. The temperature of this furnace can be varied up to 1100°C at different heating rates.

Figure 3.9 : Tabular furnace (Nabertherm GmbH) in our lab used for annealing of spectrally selective absorber films in this study.

Vacuum annealing of the spectrally selective absorber coatings are performed in a box type SS based vacuum chamber having 550 mm (width) x 450 mm (height) x 550 mm (length) dimensions. A heating arrangement is integrated with this chamber, which can be used up to 800°C at different heating rates. Digital Proportional Integral Derivative (PID) controller in conjunction with a K-type thermocouple is used to control/measure the heating system. This chamber has dynamic vacuum ~ 5 x 10^{-7} mbar, which can be monitored using microprocessor controlled pirani gauge for pressure up to 10^{-3} mbar and penning gauge form 10^{-3} to 10^{-7} mbar pressure.

3.3 SAMPLE CHARACTERIZATION TECHNIQUES

After design and development of spectrally selective coating structures, the physical, microstructural, optical, and solar thermal properties of these coatings need to be investigated. Numerous characterization techniques are used to understand the physical properties such as structural, micro-structural, elemental, optical, mechanical, thermal, corrosion and thickness of spectrally selective absorber coatings. These techniques include X-ray diffraction (XRD), Raman vibrational spectroscopy, scanning electron microscopy (SEM), energy dispersive X-ray (EDX) measurement, atomic force microscopy (AFM), UV-Vis and UV-Vis-NIR spectrophotometer, Fourier transform infrared (FTIR) spectrophotometer, nanoindentation through atomic force microscopy (AFM), Cyclic voltammetry and Tafel measurements. The basic principle of these techniques and description about the respective equipment, which is used to characterize these spectrally absorber/selective coatings are discussed in the following section.

3.3.1 X-ray Diffraction (XRD)

X-ray diffraction technique is an extremely powerful technique, used to identify the crystallinity and related crystal phases of the materials. Wilhelm Conrad Rontgen, a German Physicist, invented X-rays in 1885, which are electromagnetic radiation with 0.01 - 100 A^o wavelength ranges. Moreover, X-ray diffraction was first invented in 1912 and since it was extensively used for structural characterization, especially the crystallographic structure, crystallinity and more specifically crystallite size. The X-rays, electromagnetic radiation of short wavelength, are produced during collision between the high speed accelerated electrons and metal target. The accelerated electrons decelerate in the metal target and as a consequence generate the continuous X-ray spectrum. In this process, some of the high energy electrons knock out the innermost target electrons, generating characteristic X-rays, superimposed with continuous X-ray background.

The X-ray tube is used to generate X-rays, consists of a metal target and a thermionic electron source. The schematic of the X-ray tube is shown in Figure 3.10(a). A high voltage is applied across the electrodes to accelerate the electrons towards the target (anode). The immense cooling is used to cool the X-ray tube. Two types of X-rays are generated, continuous and characteristics X-rays. X-ray diffraction techniques normally require monochromatic radiation, known as the characteristic X-rays. Schematic illustration for characteristics X-ray generation is demonstrated in Figure 3.10(b), where innermost electron of the target material is knocked out and the created vacancy is filled with the higher orbital electron, releasing the characteristic photon of that energy difference.

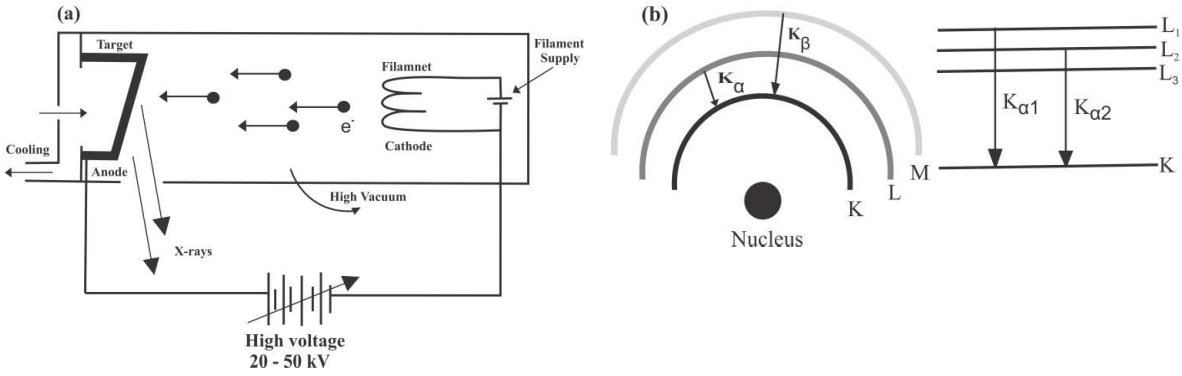

Figure 3.10 : Schematic of **(a)** X-ray tube structure and **(b)** schematic of characteristics X-ray generation. (Source: Leng, 2013)

X-ray diffraction techniques are based on wave interference. It can extract the information of inter-planar spacing using Bragg's law ($n\lambda = 2d \sin\theta$). The organization of the X-ray source, specimen, soller slit, monochromator, and detector are shown in Figure 3.11(a). The generated X-rays pass through the special soller slit and thus, a collimated X-ray beam is formed. This collimated X-ray beam through divergence slit is allowed to fall on the specimen and the diffracted beams are collected at the detector after passing through receiving slits, soller slit, and monochromator. The commonly used diffractometer is based on the Bragg-Brentano (B-B) geometry, Figure 3.11 and is suitable for thin films analysis. An additional optical arrangement is used for generating a parallel incident beam in conjunction with B-B geometry to find out the phases in thin film structures [Leng, 2013].

In this work, we used D8 Advance Powder X-ray diffractometer in conjunction with parallel beam geometry, to carry out the structural analysis of the investigated spectrally selective absorber coatings. Figure 3.12 show the D8 advance powder X-ray diffractometer system at IIT Jodhpur, used to characterize the structural properties in this study. The details of the parameters used at the time of the collecting X-ray diffraction data for the selective surface are explained in results and discussion sections in different chapters.

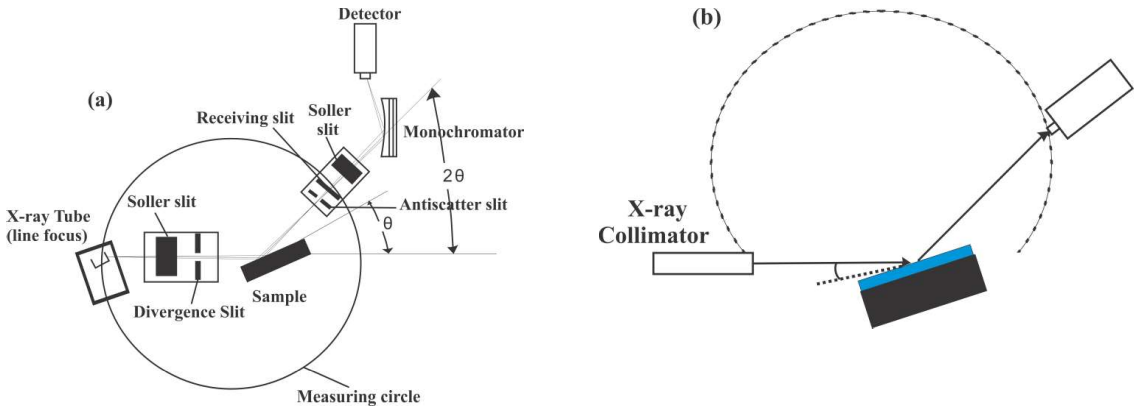

Figure 3.11 : (a) Schematic of the geometrical arrangement of X-ray diffractometer and (b) schematic of the optical arrangement of thin film diffractometer. (Source: Leng, 2013)

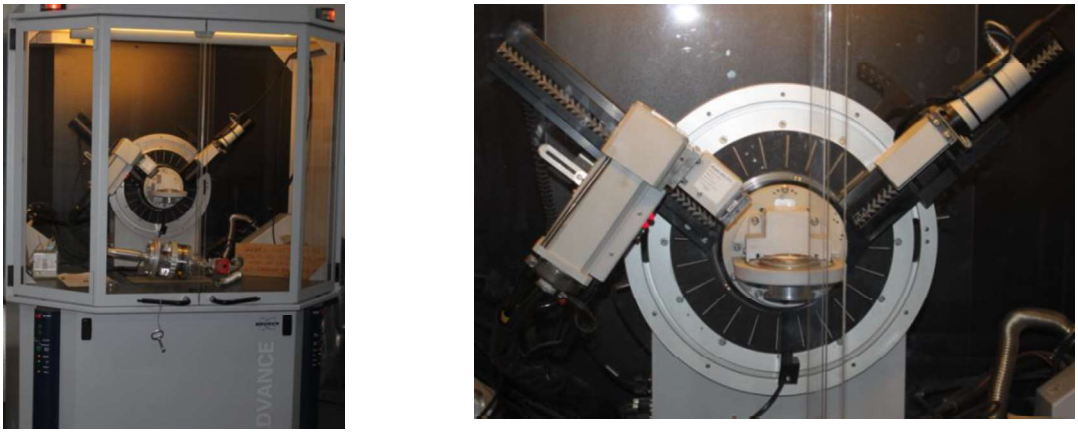

Figure 3.12 : D8 advance powder X-ray diffractometer system in our lab used to characterize the structural properties in this study.

3.3.2 Raman Vibrational Spectroscopy (RVS)

RVS is used to examine the structure of molecules using inelastic interaction between incident monochromatic electromagnetic radiation and atomic vibrations in molecules and crystal. Vibrational Spectroscopy (VS) is usually operated in the range of infrared (~ 10^{-7} m), because of probable energy range of the vibrational energy levels. Vibrational spectroscopy identifies the molecular/crystal vibrational energy levels either by absorption and/or by inelastic scattering of the incident light through a molecule/crystal.

Raman spectroscopy (RS) is based on the inelastic Raman scattering phenomenon of incident monochromatic radiation by molecules/crystals. Monochromatic radiation will be scattered both elastically and inelastically after interacting with the molecule/crystal. Elastic scattering consists of the identical frequency as that of the incident one, whereas, in the case of inelastic scattering, the scattered lights have different frequencies from that of the incident one. Inelastic scattering, in specific cases, is called Raman Scattering. There are two types of inelastic scattering processes. In one case, scattered light has more energy than that of incident light and the process is called anti-Stokes process, whereas in other, scattered light has less energy than that of incident light and the process is called Stokes process. The probability of anti-Stokes

process is much weaker than Stokes process, and that's why Raman vibrational spectrums are recorded in Stokes mode usually. Moreover, the recorded intensity as a function of change in frequency or wavenumber, is called Raman spectrum.

Molecules/crystals are made of atoms, which vibrate around their equilibrium positions. The vibrational frequencies depend on molecules/crystals atomic bonding, surrounding environment and crystallographic information. The vibrational modes are usually defined in terms of normal modes of the system, which depends on the total degrees of freedom, available to the system. Among these vibrational modes, only modes, which exhibit a change in polarizability, are Raman active and are observed in Raman vibrational spectroscopic measurements.

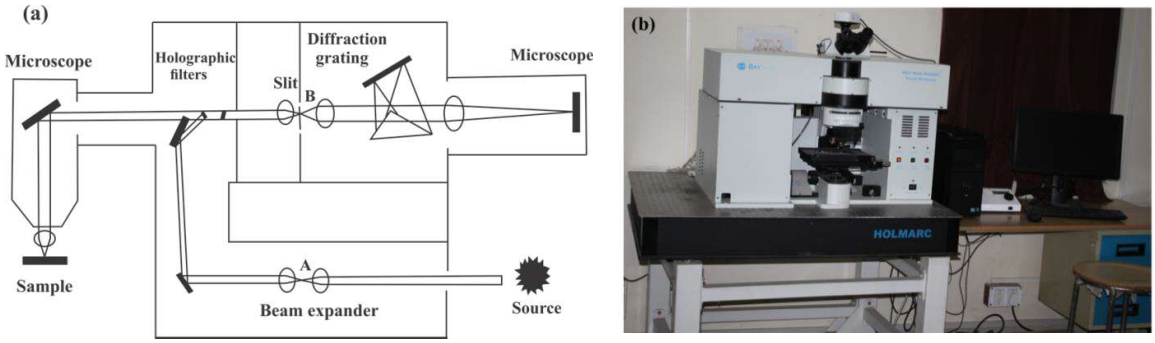

Figure 3.13 : (a) Schematic of optical diagram of Raman microscope (Source: Leng, 2013). **(b)** Nomadic Raman microscope in our lab used to measure the vibrational properties of selective absorber materials in this study.

Figure 3.13(a) illustrates the optical arrangement of a Raman vibrational spectrophotometer. A monochromatic light (mostly laser light) is focused on a sample surface using the optical microscope. The Raman scattered signals, produced due to the inelastic scattering, are too weak as compared with the Rayleigh scattered signals. Thus, a holographic filter has to be used to block the Rayleigh scattered signal and to allow the only Raman scattered signals. The wavelength dispersion of Raman scattering light is selected by a diffraction grating system before being recorded at the detector.

Nomadic™ Raman Microscope (BaySpec, USA make) has been used to analyze the vibrational properties of spectrally selective absorber coatings. Figure 3.13(b) shows the Nomadic Raman microscope at IIT Jodhpur, used to measure the vibrational properties of selective absorber materials in this study. Nomadic™ Raman microscope is equipped with multiple excitation sources (355 nm, 532 nm, and 785 nm), for Raman vibrational spectroscopy experiments. In the present study, 532 nm green monochromatic incident light source has been used. The system also consists of a dedicated spectrograph and optimized detectors for individual wavelength source to ensure optical spectral coverage, resolution, and sensitivity. It is also featured with integrated laser control and motorized ND filters for attenuating laser power. A fully functional Olympus microscope is integrated with motorized stage provides a 3"x 2" platform for transmittance and reflectance mode operation. Moreover, a CCD camera is equipped on the top of the microscope for capturing bright field image. Details of the experiments are given in results and discussion section of chapter 5.

3.3.3 Scanning Electron Microscope (SEM)

Scanning electron microscope (SEM) is used to probe the microscopic structure, more precisely the surface structure, by scanning across the surface. The essential components of SEM are an electron gun, series of electromagnetic lenses and apertures. Figure 3.14 (a) shows the schematic skeleton of a SEM. The electromagnetic lenses are used for collimated electron beam formation and the objective lenses are used to focus the electron beam as a nanometer diameter probing electron beam. Probe scanning is carried out by using the beam-deflection system, integrated within the objective lens of the SEM. The deflection system of the electron probe is controlled by pairs of electromagnetic coils (also called scanning coils). Apertures are mainly used for limiting the divergence of the electron beam in its optical path.

To obtain a good SEM images, it is essential to control the operational parameters to get the desired depth of field (DoF) and resolution. The DoF is strongly affected by the working distance and aperture size. Resolution of the images is adjusted by the two operational variables (i) the acceleration voltage of electron gun and (ii) probe current. Astigmatism is another operational variable, and needs to minimize for better microscopic information. These parameters become significant at higher resolution and need to be adjusted properly to get the clear scanning electron microscopic images.

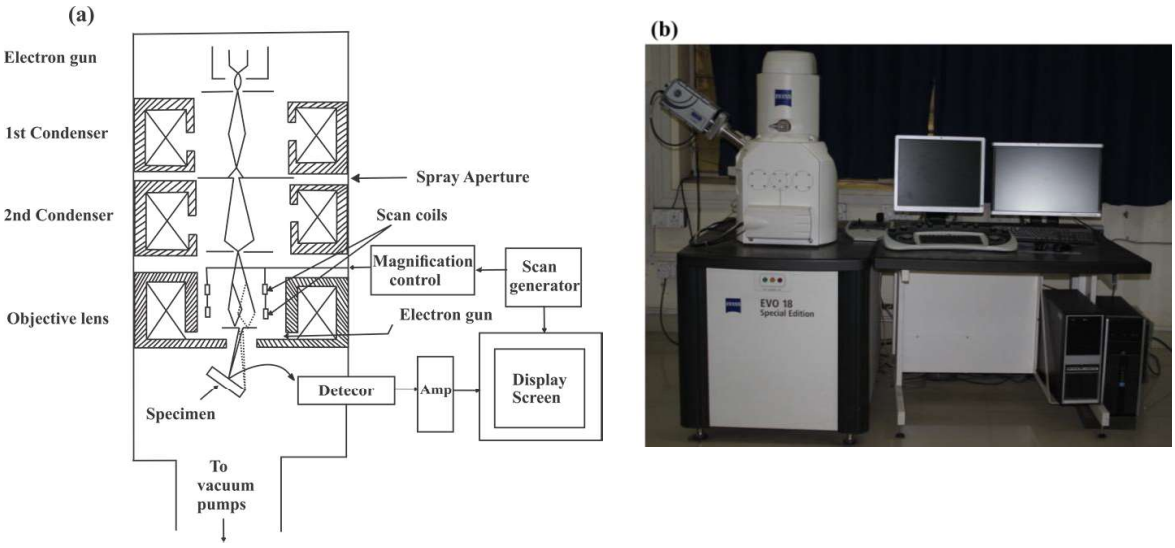

Figure 3.14 : (a) Schematic of the structure of a scanning electron microscope (SEM) (Source: Leng, 2013). **(b)** Carl Zeiss scanning electron microscope system conjunction with EDS in our lab used to characterize the surface properties and elemental analysis of selective absorber films.

Carl Zeiss SEM EVO 18 special edition has been used to analyze the surface and cross-sectional morphologies and grain sizes of the spectrally selective absorber materials. Figure 3.14(b) shows Carl Zeiss scanning electron microscope system in conjunction with an energy dispersive spectroscopy (EDS) accessory at IIT Jodhpur, used to characterize the surface properties and elemental analysis of selective absorber films.

3.3.4 X-ray Energy Dispersive Spectroscopy (EDS)

EDS is an X-ray spectroscopy technique. It uses characteristics X-rays to identify chemical elements in a material. EDS is generally an add-on component with electron microscopes such as SEMs and transmission electron microscope (TEMs). Oxford makes (X-act) EDS instrument is attached with Carl Zeiss SEM EVO 18 special edition, as shown in Figure 3.14 (b). This is used to evaluate the elemental compositions in spectrally selective absorber materials coatings used in this thesis work.

3.3.5 Atomic Force Microscope (AFM)

AFM is a popular member of scanning probe microscopy (SPM), which is invented in late 1980s. AFM uses near-field forces between atoms of the probe tip apex and surface to generate signals for surface topography, Figure 3.15(a) shows the schematics of AFM. A probe tip, which is mounted on a cantilever spring, used to scan the surface. Near field forces between the tip and the sample surface are detected using a beam-deflection system, which senses the respective spacing. The main part of AFM, which differentiates it with other SPM members, is its microscopic force sensor. Normally, AFM is operated in two modes: (i) static, and (ii) dynamic. Static mode must be operated in a contact type, whereas, dynamic modes may be operated in both contact and non-contact types [Leng, 2013; Wiesendanger, 1994; Zhang *et al.*, 2009; Butt *et al., 2005*].

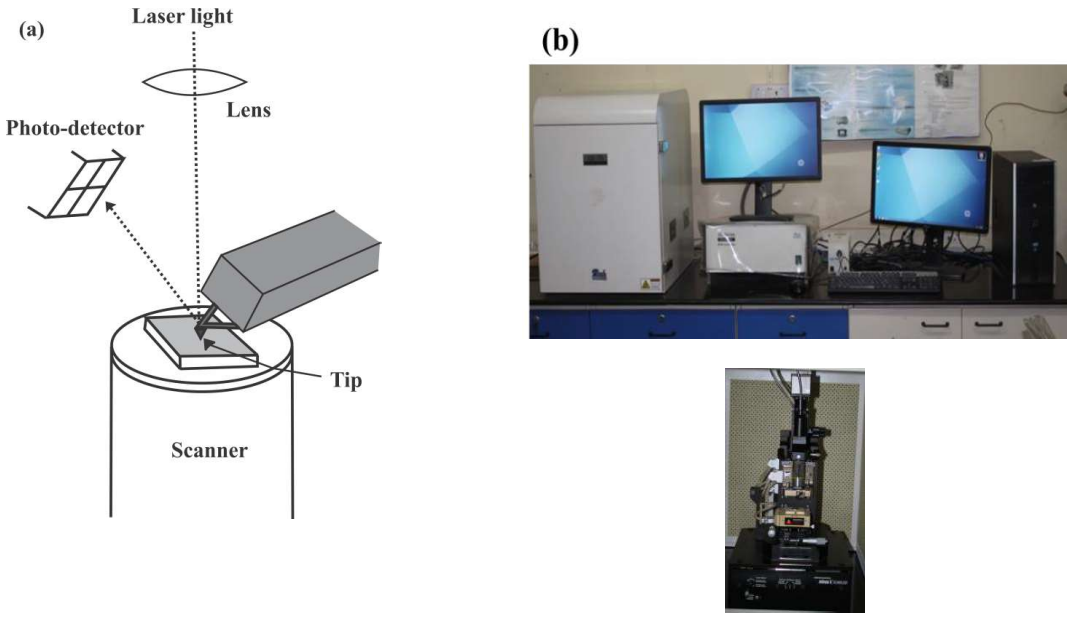

Figure 3.15 : (a) Schematic of an atomic force microscopy (AFM) (Source: Butt, 2013). **(b)** Scanning probe microscopy (SPM) instruments in our lab used to analyze surface parameters in this study.

A Park System, scanning probe microscopy (SPM), XE-70 has been used to analyze the surface morphologies, surface roughness, grain size and in some cases the thickness of spectrally selective absorber coatings. Figure 3.15 (b) shows scanning probe microscopy (SPM) instruments, at IIT Jodhpur, used to analyze surface parameters in this study. Details of the AFM experiment will be presented in results and discussion part wherever AFM results are presented.

3.3.6 Profilometer (Thickness Measurements)

A Profilometer is a device used to measure the roughness of the surfaces. It provides the relative difference between a high and low point on a surface in nanometres to micrometer range. A stylus (sharp tip) based Profilometer traces the surface with a stylus and records the tip position using optical or electrochemical methods [Conroy and Armstrong, 2006]. A stylus Profilometer contains a stylus, which is in contact with the surface of samples and an electrochemical transducer that converts its Z coordinate into voltage. An amplifier and analog-to-digital converter are connected to a computer to record measurements [Leach, 2001]. DektakXT stylus profiler has been used to measure the thickness of the spectrally selective films, coated on different substrates (Fig. 3.16).

Figure 3.16 : DektakXT stylus profiler at IIT Jodhpur, used to measure the film thickness of spectrally selective absorber coatings in the present study.

3.3.7 Optical Measurements

The optical properties of spectrally selective absorbers are commonly examined using spectrophotometers in the desired wavelength ranges. UV-Vis-NIR spectrophotometers are of special interest, which can cover the entire solar spectrum (0.2 – 2.5 μm). In contrast, UV-Vis spectrophotometers cover around 50% of the wavelength range of the solar spectrum (0.2 - 0.9 μm) only and completely exclude the infrared part of the solar spectrum. Thus, it is important to use UV-Vis-NIR spectrophotometer to understand the complete spectral response of spectrally selective coatings.

Fourier transform infrared (FTIR) spectrophotometers cover the infrared 2.5 – 25 μm region. This range is important to understand the materials optical/thermal properties, especially emissivity, and may be considered as feedback for the development of desired physical properties. In this section, the basic principle of spectrophotometer techniques, used to measure the optical properties (absorptance and emittance) of selective absorbers materials will be discussed.

3.3.7.1 UV-Vis-NIR/ UV-Vis Spectrophotometer

Agilent technology Cary 5000 UV-Vis-NIR spectrophotometer is used to collect the total and diffuse reflectance, which covers 0.175 – 3.3 μm wavelength range, thus entire solar spectral range. This UV-Vis-NIR spectrophotometer is a double beam system, equipped with a photomultiplier detector for the UV-Vis range and PbS detector for NIR range. A 150 mm diameter integrating sphere accessory, an external DRA, has been used in normal scan mode to get the reflectance in the desired wavelength range. The external DRA system can be combined with the main instrument. The integrating sphere is an optical device used to collect and

measure electromagnetic radiation from an object. The integrating sphere is coated with a 4 mm thick polytetrafluoroethylene (PTFE), a white diffusive material and fitted in the same detector configuration as the main spectrophotometer during diffuse reflectance experiments. The reflectivity of the PTFE is above 96% between 0.2 – 2.5 µm, and greater than 99% between 0.3 – 1.8 µm. Figure 3.17 (a) shows the schematic view of external DRA and optical design view of the external DRA (b), used to measure the total reflectance of spectrally selective absorbers for the present work.

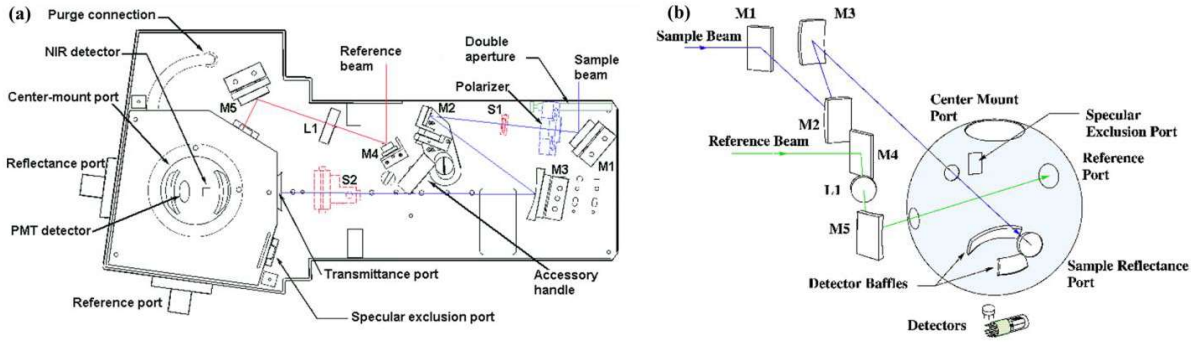

Figure 3.17 : (a) A schematic view of the external DRA and **(b)** the optical design view of the external DRA used to measure the total reflectance of spectrally selective absorbers in this study. (Source: Manual of Cary 5000 VU-Vis-NIR, Agilent Technology)

In DRA measurements, a baseline is collected first using the PTFE reference disk, and then the sample is mounted over the sample reflectance port and the diffused reflection of the sample is collected by the integrating sphere. The solar absorptance, α, of the selective absorbers, is calculated by measuring the total reflectance in the solar wavelength range and weighting by 1.5 AM solar radiation using Equation (2.5).

In this study, Cary 4000 UV-Vis spectrophotometer has also been used to collect the total reflectance of selective absorbers in the range of 0.2 – 0.9 µm. This equipment has only the photomultiplier (PMT) detector and NIR region is not available. This spectrophotometer is also equipped with 110 mm diameter integrating sphere for DRA measurements. The integrating sphere can be easily installed using the lock down mechanism in the sample compartment of the instrument. Figure 3.18 represent the schematic view of the optical design of the internal DRA (left) and beam diagram when the sphere is kept in the D (middle) and S (right) positions of the accessory. If accessory is kept in the D position, the detector only detects the diffuse reflectance. However, in S position, the detector can collect total reflectance including the specular one as well.

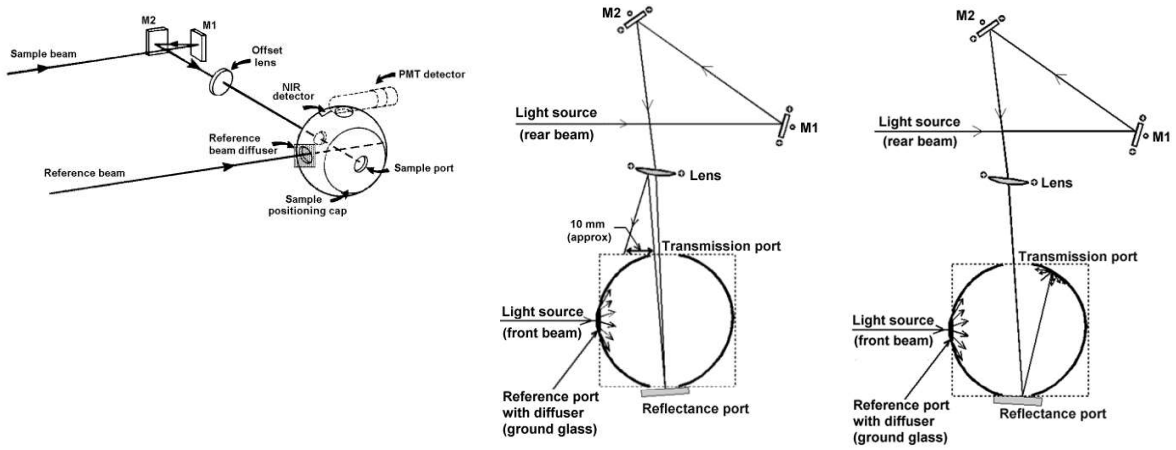

Figure 3.18 : A schematic view of the optical design of internal DRA **(Left),** beam diagram of the accessory with the sphere cap in the D position **(middle)** and beam diagram of the accessory with the sphere cap in the S position **(right).** (Source: Manual of Cary 4000 VU-Vis spectrophotometer, Agilent Technology)

3.3.7.2 Fourier Transform Infrared Spectrophotometer (FTIR)

FTIR has extensively been used for vibrational spectroscopic measurements. It depends on the interaction of infrared radiation with the vibrating dipole moments of molecules. Reflectance spectra of the spectrally selective absorbers are recorded in 2.5 – 25 μm wavelength range to understand the infrared/thermal response of these coatings. We used a Bruker FTIR spectrometer vertex 70v and snap of the same is shown Figure 3.19. This spectrometer consists of a room temperature Deuterated and L-alanine doped Triglycine sulfate (DLaTGS) detector. The resolution of this FTIR spectrophotometer is ~ 0.4 cm^{-1}.

Figure 3.19 : Bruker FTIR spectrometer vertex 70v in our lab used to collect the reflectance spectra of spectrally selective absorbers.

FTIR 70v spectrometer has a fully evacuated optical bench, which is used to remove the residual environmental background such as gases, moistures etc. during the experiments. A 30 degree fixed angle specular reflectance accessory, as shown in Figure 3.20, has been used to collect the reflectance spectra of the spectrally selective absorbers. The sample is placed on the hole in the attached platform, as explained in Figure 3.20. The background spectrum is collected by using a gold coated reference sample, as an ideal reflector, for the infrared region. The FTIR

instrument is used to collect the total specular reflectance in 2.5 – 25 μm wavelength range and the thermal emittance has been calculated from these measurements using Equation (2.7).

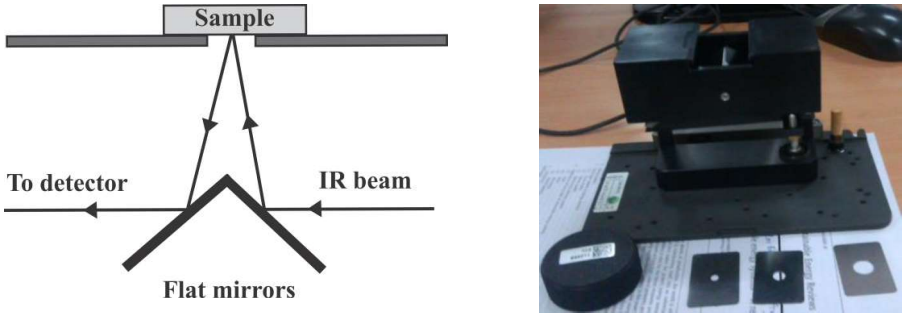

Figure 3.20 : (Left) Optical diagram of fixed angle (30 degrees) specular reflectance accessory (Source: Leng, 2013). **(Right)** 30 degree horizontal fixed angle specular reflectance accessory.

3.3.8 Thermal Analysis

Thermal analysis is an analytical technique that measures the properties or change in properties of materials as a function of temperature. There are several common thermal analysis techniques such as thermogravimetry (TG), differential thermal analysis (DTA), and differential scanning calorimetry (DSC). TG is particularly employed to check the decomposition of materials by invigilating the mass change as a function of temperature. DTA and DSC are widely used to analyze the phase change as a function of temperature for the different materials [Leng, 2013]. Figure 3.21 shows the schematic diagram of a thermal analysis instrumentation, which consists of the sample with control heating option in conjunction with high precision weighing balance. The systems are usually automated/interfaced with a computer for data logging and analysis.

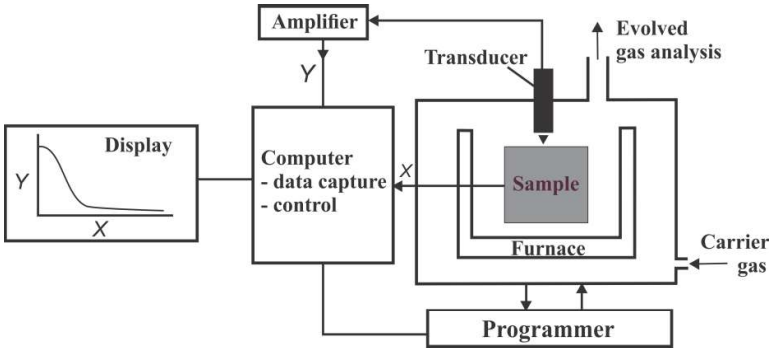

Figure 3.21 : Schematic of the general instrumentation of thermal analysis. (Source: Leng, 2013)

The key component of the TG instrument is the microbalance, which measures the change in mass of the sample. Figure 3.22 (a) shows the schematic of a null-type microbalance (commonly used), also called the Cahn microbalance. TG analysis mostly relies on the mass of the sample. Normally, a small amount of the sample is better with respect to the large amount to minimize the temperature inhomogeneities across the sample during the measurements. Moreover, the mass of the sample is usually about several milligrams. TG measurements can be done in both reactive and non-reactive atmosphere. The non-reactive atmosphere should be

created using an inert gas. Normally, argon (Ar) and nitrogen (N_2) gases are used for creating nonreactive atmospheric conditions. This (TGA) is a simple and effective technique to estimate thermal stability and chemical reactions by monitoring mass change for materials of interest [Leng, 2013]. In order to measure the thermal stability of spectrally selective absorber materials, the simultaneous thermal analyzer (STA) is used. STA 6000 is used to measure TG responses for different coating structures. Figure 3.22 (b) shows a Perkin Elmer simultaneous thermal analyzer 6000 (STA 6000) at IIT Jodhpur, used for thermal gravimetric measurements of spectrally selective absorber films. The instrument is equipped with a top loaded furnace, where temperature can be varied from 15 °C to 1000°C at different heating scan rates from 0.1 to 100°C/min with sample capacity of ~ 1500 mg. Balance sensitivity of 6000 STA is of the order of 0.1 µg.

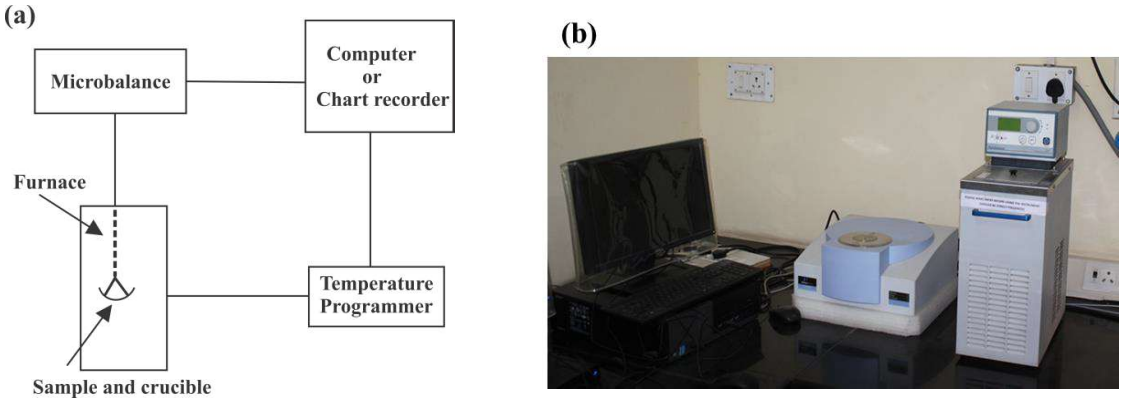

Figure 3.22 : (a) Schematic of commonly used null-point type microbalance. (Source: Leng, 2013) **(b)** Perkin Elmer simultaneous thermal analyzer 6000 (STA 6000) in our lab used for thermal annealing of spectrally selective absorber films.

3.3.9 Mechanical Characterization

Mechanical properties, such as Young's modulus (YM) and hardness, of spectrally selective absorbers, are measured using nanoindentation method. The nanoindenter, which is used in this study, is an integrated accessory with atomic force microscopy (scanning probe microscopy (SPM) XE-70, Park) system. In this study, the indenter, used for measurement, is a Berkovich indenter, and made of a sapphire cantilever attached with a diamond tip. Tip stiffness, radius, height, thickness, and length are 140 N/m, <25nm, 96µm, 26µm, and 717µm. The respective frequency, half angle, front angle, side angle, inclination values for the tip are 52 kHz, 30°, 90°, 79°, 12°, respectively. Oliver and Pharr analysis has been used to calculate the hardness and YM of spectrally selective absorbers [Oliver and Pharr, 1992, 2004]. The key parameters, used to analyze the hardness and Young's modulus, are the maximum load, P_{max}, the maximum displacement, h_{max}, and the elastic unloading stiffness, S = dP/dh, defined as the slope of the upper portion of the unloading curve during the initial stages of unloading. From the analyzed load-displacement curves, Young's modulus can be calculated using equation (3.4).

$$\frac{1}{E_{eff}} = \frac{2\beta}{S}\sqrt{\frac{A}{\pi}} = \frac{1-\nu_s^2}{E_s} + \frac{1-\nu_i^2}{E_i} \quad , \tag{3.4}$$

where A, E_{eff}, S, and β are the actual contact area, effective (or reduce) modulus for each indenter/specimen combination, measured stiffness and a shape constant (β) which is 1.034 for for Berkovich tip [Fang et al., 2004]. E and ν represent Young's modulus and Poisson's ratio of the indenter (i) and the sample (s) respectively. The values used for Poisson's ratio ν and

Young's modulus E_i for diamond indenter is 0.07 and 1141 GPa [Oliver and Pharr, 1992]. Hardness values can be calculated using equation (3.5) [Oliver and Pharr, 1992, 2004], where A is the effective area of contact.

$$H = \frac{P_{\max}}{A} \tag{3.5}$$

The details of the nanoindentation measurement parameters in this study are discussed in respective chapters.

3.3.10 Electrochemical Measurements

Electrochemical measurements, such as cyclic voltammetry (CV) and linear sweep voltammetry (LSV), are used to understand the chemical response of a system under an electrical excitation (stimulation). This section covers CV and LSV electrochemical techniques, which are used to understand the oxidation, reduction and corrosion response of spectrally selective absorbers in this study.

3.3.10.1 Cyclic Voltammetry (CV)

CV is an extensively used electroanalytical technique for electrochemical measurements. In this technique, the potential difference between working and the reference electrode is swept linearly in time from a start potential to a final potential, and reversed to complete a cycle. The current response of a small stationary electrode in unstirred solution is excited by a triangular potential waveform (Fig. 3.23 (a)). The waveform produces the forward and reverse scans. The resulting current at the working electrode is collected against the applied electrode potential in voltammogram. Figure 3.23 (b) illustrates the respective response of a reversible redox couple during a single potential cycle [Wang, 2006; Skoog *et al*., 2004; Kissinger and Heineman, 1996].

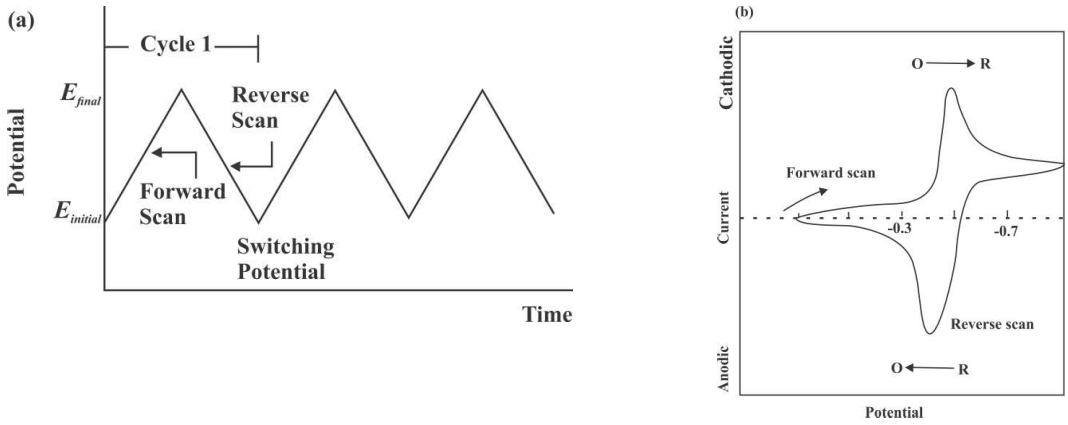

Figure 3.23 : (a) Potential-time excitation signal in a cyclic voltammetric experiment. **(b)** Typical cyclic voltammogram for a reversible redox process. (Source: Wang, 2006)

The mostly used experimental configuration for collecting CV consists an electrochemical cell system (Figure 3.24 (a)), with three electrodes: (i) counter or auxiliary, (ii) reference, and (iii) working electrode. These electrodes are dipped in a liquid electrolyte and connected to a potentiostat. A potentiostat is used to measure the potential difference between the reference and working electrode. A counter electrode with this configuration is used for accurate current measurements between the WE and RE. Counter electrode plays an important

role to ensure that no current is passing through the reference electrode and potential across the reference electrode remains constant during the measurement.

In this study, Iviumstat electrochemical workstation (Figure 3.24 (b)) has been used to measure CV response for spectrally selective absorbers films coated on several substrates, such as copper, stainless steel, aluminum etc. Ag/AgCl electrode and platinum wire electrode are used as reference and counter electrode. The selective absorber films coated substrates (Cu, SS, Al) are used as working electrode. 3.5 wt% NaCl saline solutions are used as the electrolyte for accelerated evaluation of corrosion properties. To understand the CV response of interested structures, the experiments are carried out at several scan rates and several cycles, the details of such experiments and related results are discussed in respective sections.

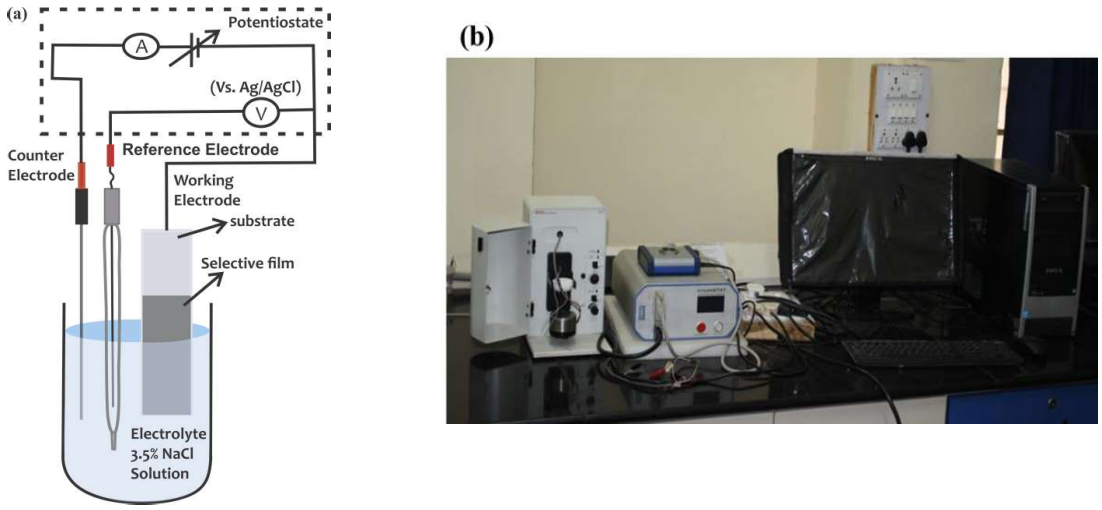

Figure 3.24 : (a) Schematic of the experimental setup for cyclic voltammetry experiments with three electrode configuration. **(b)** Iviumstat electrochemical workstation in our lab used to form the electrochemical measurements of spectrally selective absorber coatings.

3.3.10.2 Corrosion Measurements

Corrosion is the degradation of materials by means of chemical reactions under environmental conditions, in which the material is used for possible applications. Linear sweep voltammetry is used for corrosion studies, in which potentiodynamic polarization measurements are carried out to measure the corrosion measurement of the spectrally selective absorber films coated on the substrate. In a linear sweep measurement, potential across the working electrode is varied at a constant rate throughout the scan and resulting current is measured.

To perform the polarization measurements, an electrochemical three-electrode (working, counter and reference) test setup, integrated with a potentiostat has been designed and used for corrosion experiments (Figure 3.25). Working electrodes, whose potential is varied linearly with time, versus a reference electrode, are spectrally selective structures in the present studies. The potential at reference electrode is kept constant throughout the experiments. The current is measured between the WE and CE. These measurements are used for Tafel analysis to estimate the corrosion resistance (R_P), corrosion current density (i_{corr}) and corrosion potential (E_{corr}) relative to reference electrode by extrapolating the straight line portions of the anodic and cathodic lines.

The corrosion currents are determined using Tafel plot analysis to understand the corrosion rates of these spectrally selective coatings. The Butler-Volmer (B-V) equation (Equation 3.6) gives the relation between the current density i and the charge transfer overpotential η, in terms of exchange current density i_0, and transfer coefficient α [Paunovic and Schlesinger, 2006].

$$i = i_0\left[\exp\left(\frac{(1-\alpha)zF\eta}{RT}\right) - \exp\left(-\frac{\alpha zF\eta}{RT}\right)\right] \quad , \tag{3.6}$$

where $F = eN$ *is* Faraday constant, z is a number of electrons, R is the gas constant and T is the absolute temperature. When an electrode is a part of an electrochemical cell through which current is flowing, the overpotential, η, is defined as the difference between applied potential and corrosion potential E_{corr}.

$$\eta = E - E_{corr} \tag{3.7}$$

E_{corr} is open circuit potential of the corroding materials and also termed as corrosion potential.

For large anodic current (η has large values) the B-V equation simplifies to the Tafel equation for the anodic reaction (Equation 3.8):

$$\eta = \log i_{corr} + b_a \log i \tag{3.8}$$

Where, b_a is the anodic Tafel slope.

$$\log i_{corr} = -\frac{(a(1-\alpha)zF)}{2.303RT}; b_a = \frac{2.303RT}{(1-\alpha)zF} \tag{3.9}$$

For large cathodic current (η has large values) the B-V equation simplifies to the Tafel equation for the cathodic reaction (Equation 3.10):

$$\eta = \log i_{corr} - b_c \log|i| \tag{3.10}$$

Where b_c is the cathodic Tafel slope.

$$\log i_{corr} = -\frac{a\alpha zF}{2.303RT}; b_c = \frac{2.303RT}{\alpha zF} \tag{3.11}$$

The corrosion current, i_{corr}, anodic Tafel slope, b_a, and cathodic Tafel slope, b_c, can be measured from the experimental data. Stern-Geary equation [Stern an Geary, 1957] can be used to calculate corrosion current density, i_{corr}, which is as follow;

$$i_{corr} = \frac{b_a b_c}{2.3R_p(b_a + b_c)} \tag{3.12}$$

Where b_a and b_c are Tafel slopes and *Rp* is the polarization resistance. Finally, corrosion rate can be calculated using the following equation:

$$\text{Corrosion Rate (mpy)} = \frac{0.13\ i_{corr}\ (\text{E.W.})}{d} \tag{3.13}$$

Where, E.W. is equivalent weight of the corroding material in gram. d = density of the corroding material, in g/cm^3, and i_{corr} = corrosion density in μA/cm^2 and mpy is mils per year or mils penetration per year [Fontana, 2009].

In this study, Tafel analysis is used to measure the corrosion response of spectrally selective absorber films coated on several substrates. Schematic setup of corrosion measurements is illustrated in Figure 3.24 (a) with right panel showing the electrochemical experimental setup, used to perform the corrosion measurements in this study. The details about corrosion behavior on different spectrally selective structures are discussed in respective sections.

…